Attachment A

INTERGRANULAR CORROSION CRACKING OF TYPE 304 STAINLESS STEEL IN WATER-COOLED REACTORS

C. F. Cheng

Materials Science Division
Argonne National Laboratory
Argonne, Illinois 60439

Table of Contents

INTERGRANULAR CORROSION CRACKINC OF TYPE 304 STAINLESS STEEL IN WATER-COOLED REACTORS*

C. F. Cheng

Materials Science Division
Argonne National Laboratory
Argonne, Illinois 60439

ABSTRACT

Nuclear pressure vessels, primary piping, core components, and fuel-element cladding are subject to cyclic thermal and mechanical stresses due to the high pressure and temperature of the coolant or of the fuel. When Type 304 stainless steel is used as material for these parts, potential intergranular corrosion failures due to the combined action of corrosion and low-cyclic stress or high static stress need critical evaluation. This paper reviews Type 304 stainless steel with respect to (a) the instances of service failure in water-cooled reactors, (b) the various corrosion studies on intergranular cracking, and (c) the proposed mechanisms of intergranular corrosion cracking.

1. Introduction

Nuclear pressure vessels, primary piping, core components, and fuel-element cladding are subject to cyclic thermal and mechanic stresses due to the high pressure and temperature of the coolant or of the fuel. When Type 304 stainless steel is used as material for these parts, potential intergranular corrosion failures due to the combined action of corrosion and low-cyclic stress or high static stress need critical evaluation. Numerous instances of such intergranular corrosion cracking of austenitic stainless steel (Types 304 and 304L) have been observed in U. S. nuclear reactors. In boiling water reactors, service failures have been reported in a variety of components, including fuel-element cladding,[1,2] preheater pipes,[3] and vessel liners.[4] In pressurized water reactors, failures of fuel-element cladding[5] and outlet nozzles[6] have been reported. These failures have occurred in both metallurgical conditions; sensitized and solution annealed. The mode of cracking is exclusively intergranular. However, none of the cracking instances is associated with either chloride or caustic solution. This paper discusses austenitic stainless steel with respect to:

(a) the instances of the above-mentioned failures,

(b) the various corrosion studies on intergranular cracking, and

(c) the proposed mechanisms of intergranular corrosion.

2. Instances of Service Failure

Instances of intergranular corrosion cracking of austenitic stainless steel (Types 304 and 304L) in water-cooled reactor service are briefly discussed below:

2.1 Boiling Water Reactors (BWR)

In boiling water reactors, the primary coolant is high-purity water at a temperature of about 286°C. The water normally operates at neutral pH (∿ 7) with a resistivity of approximately 1 MΩ-cm total solids from 1 to 10 ppm, chloride of about 0.02 ppm, and oxygen from radiolytic decomposition up to 0.3 ppm in the water and from 10 to 20 ppm in the steam.[5] In-service intergranular fractures have been reported in two BWR. These reactors are located at Vallecitos, California and Dresden, Illinois.

2.1.1 Vallecitos Boiling Water Reactors (VBWR)

Type 304 stainless steel tubing with outside diameter and wall thickness ranging from 0.914 to 1.07 cm (0.360 to 0.420 in.) and from 0.020 to 0.051 cm (0.508 to 0.020 in.), respectively, were tested as fuel-element cladding in VBWR.[7] About 40 out of the 900 rods exhibited intergranular failures in 500-1000 hr. However, no carbide precipitate could be seen at the grain boundaries by means of either light or electron microscopy. The cracking patterns varied with the initial condition of the tubing. Cracks in the cold-worked tubings were mostly longitudinal, whereas those in the annealed condition were predominantly circumferential. A statistical analysis of the failure-rate data indicated the following:

(a) There was no significant difference in failure rate between solution annealed and cold-worked cladding.

(b) The failure rate of "collapsed cladding" was significantly higher than for "free-standing cladding" (indicating the influence of cyclic stress).

(c) Fuel rods that operate at high surface heat fluxes (e.g., > 95 W/cm^2 or 3×10^5 $BTU/hr/ft^2$) showed an increased failure rate over fuel rods that operate at lower heat fluxes.

2.1.2 Dresden-I Boiling Water Reactor (Dresden-I BWR)

Type 304 stainless steel fuel-element cladding exhibited longitudinal intergranular cracking in Dresden-I BWR.[8] The tubing used was commercially annealed and then cold rolled to 1.242 cm (0.489 in.) outside diameter. The tubing ranged from 0.025 to 0.043 in. in wall thickness. The cladding was subject to an average exposure of 95 W/cm^2 (3×10^5 $BTU/hr/ft^2$) peak heat flux. Since the cladding was "nonfree" standing and the failure occurred only at the highest heat flux region, it was concluded that stress was a strong contributor to the cracking mechanism. Fluence was not a factor, since simulated ex-reactor tests showed similar failure phenomena for other 18 wt% Cr-8 wt% Ni austenitics as well. Furthermore, studies conducted by Hazelton et al.[9] on UO_2 fuel rods clad with Type 304 stainless steel showed irradiation produced only slight structural changes of the cladding at similar fluence, but no increase in susceptibility to intergranular corrosion (as indicated by post-test exposure to acidified copper sulfate colution). Irradiation exposures ranged from 1.7×10^{20} to 9.8×10^{20} cm^2 (> 1 MeV).

Preheater pipes of small diameter (6 in. or less) also suffered weld defects and leaking cracks in Dresden-I BWR.[3] The coolant leaks that occurred in Type 304 stainless steel tubing (Schedule 80) were

circumferentially oriented cracks. The typical crack lengths were from 2 to 4 in. long. These cracks initiated at the inner surface of the pipe in the counterbored fit-up region adjacent to the welds. Metallographic examination revealed the mode of cracking was exclusively intergranular. The microstructure surrounding the cracks showed grain-boundary carbide precipitation during welding. The cracking was restricted to the heat-affected zones of the pipe base metal. The crack propagation initiated from a single gamma (γ) austenite phase of base metal of Type 304 stainless steel and arrested at the two-phase austenite plus delta ferrite ($\gamma + \delta$) weldment of Type 308 stainless steel. However, no indication of cracking was observed in any of the large diameter (greater than 6 in.) piping. The small-diameter pipe was welded with a procedure that uses a high heat input and low number of passes, and the large-diameter piping was welded by using a low heat-input and multiple passes. The latter procedure produced less carbide precipitation than the former.

2.2 Pressurized Water Reactors (PWR)

In pressurized water reactors, the primary coolant is also high-purity water. The pH of the coolant, in some applications, is maintained in the range of from 9 to 10.5 by the addition of lithium or ammonium hydroxide. In addition, hydrogen is added to suppress the oxygen formed from radiolytic dissociation of water. Intergranular cladding failure of austenitic stainless steel in both sensitized and solution annealed conditions has been reported in pressurized water reactor service.

2.2.1 PWR Test Loops

One experiment conducted in Engineering Test Reactor (ETR) loop was prematurely terminated as a result of release of excessive fission product.[10] It was determined that a pump failure and subsequent loss of coolant were responsible for the severe thermal conditions which cracked a fuel-rod cladding to produce the "fission break". The fuel rods had operated for 76 days in 600°F lithiated water at pH 10 and at peak surface heat flux of 93 W/cm^2 (296,000 $BTU/hr/ft^2$). The UO_2 pellets were clad in Type 304L stainless steel tubing that had a diameter of 0.820 cm (0.332 in.). The stretch-formed fuel rod with 0.038-cm (15 mil) wall tubing suffered intergranular cracking, while the free standing fuel rod with 0.053-cm (21 mil) wall was only dimensionally distorted. The severe thermal condition also changed the cladding from a solution annealed to sensitized structure. The cladding failure of the stretch-formed fuel rod was attributed to stress rupture in conjunction with hydrogen under the severe thermal conditions. The hydrogen was generated by the reaction of the UO_2 fuel and water.

Knolls Atomic Power Laboratory (KAPL) reported intergranular cracking of vacuum-annealed Type 304L stainless steel cladding on poison elements used in test pressurized water reactors.[5,11] The failure occurred during irradiation in 600°F ammoniated water at pH 10 when the cladding was stressed in excess of the yield point. The hydrogen content of the irradiated cladding increased from 4-6 ppm to 8-14 ppm in 700 effective full-power hours. Stress rupture cracking aided by hydrogen was indicated.

2.2.2 Savannah River Reactor

Intergranular stress corrosion cracking was detected in two Type 304 stainless steel nozzles in the high-purity heavy-water moderator of the Savannah River Reactor Plant.[6,12] The cracks propagated from surface intergranular attack at sensitized grain boundaries. The attack was the result of acid ($HF-HNO_3$) pickling during initial fabrication of the nozzles. Cracking was attributed to chlorides although the bulk water contained only 0.006 ppm chloride. Fluoride contamination is more likely. Recent studies[13] reported that fluoride ions with a concentration below 1 ppm in bulk water can result in intergranular cracking at the crevices of sensitized Type 304 stainless steel (see sections 3.1.3 and 3.1.4).

3. Corrosion Studies on Intergranular Cracking

The service failures noted in Section (2.) are associated with one of the following two conditions:

(a) impurities in aqueous solution, and

(b) embrittlement and irradiation effects.

We shall review laboratory studies on intergranular corrosion cracking under these conditions.

3.1 Impurities in Aqueous Solutions

3.1.1 Nitric-Dichromate Solution

Sensitization is not a prerequisite for intergranular corrosion of Type 304 stainless steel. Nonsensitized steel will also corrode intergranularly when exposed to certain chemical environments. Accelerated

corrosion of nonsensitized stainless steel during exposure to boiling nitric acid was reported as early as 1952 by DeLong[14] and later by Shirley and Truman.[15] These workers attributed this accelerated corrosion to the presence of chromium ions that had been dissolved from the test specimens. Others[16,17] have shown that dissolved chromium in nitric acid can accelerate intergranular attack only when the chromium is at the highest oxidation state, Cr^{+6}.

It was not until 1959, however, that Streicher[18] reported that the accelerated corrosion of nonsensitized stainless steel in nitric-dichromate solutions resulted in preferential grain-boundary attack. In addition to Cr^{+6}, the following ions have been found to activate intergranular corrosion of nonsensitized stainless steel in nitric acid solutions: Mn^{+7} (MnO_4^{-1}), Ce^{+4}, and Fe^{+3}[18,19]. The kinetics of intergranular corrosion of nonsensitized stainless steel in nitric-dichromate solutions have been studied with respect to several environmental variables. Various workers have shown that the rate of intergranular attack increases with corresponding increases in HNO_3 concentration, Cr^{+6} concentration, solution temperature or specimen stress level.

Metallurgical variables that have been studied to date include (a) grain size of austenitic stainless steel, (b) cold work, (c) surface treatment, (d) alloy composition, and (e) heat treatment in nitric-dichromate solutions. Coriou, et al.[19] and Armijo[20] have studied the effects of grain size and cold work. They reported that the rate of intergranular penetration increases as the grain size increases, and decreases with an increase of cold work. The effects of these variables

are small; for example, a tenfold increase in grain size will result in only a twofold increase in intergranular corrosion rate. Similarly, a 50 percent reduction in thickness (by rolling) will produce only a twofold decrease in corrosion rate. Warzee and Berge[21] have found that superficial cold work reduces the rate of intergranular corrosion. This surface working is effective in reducing the corrosion of both sensitized and nonsensitized alloys. Armijo[22] found that high-purity Fe-Cr-Ni alloys (14 wt% Cr-14 wt% Ni-balance Fe) are immune to intergranular corrosion. The addition of impurities such as C, N, O, Mn and S does not promote intergranular corrosion susceptibility of a nonsensitized high-purity Fe-Cr-Ni alloy. However, the addition of Si and P will promote severe susceptibility. Furthermore, the removal of Si and P from austenitic alloys of commercial purity decreases susceptibility to intergranular corrosion by a factor of six to eight. The effect of heat treatment has been extensively evaluated by Aust[23] to support the solute segregation theory (see Section 4). He reported that Type 304 stainless steel specimens quenched from high temperatures (1300°C) were more susceptible to intergranular corrosion than specimens quenched from temperatures between 1200 and 900°C. Also, specimens stabilized at 800-900°C were more resistant to attack than solution-annealed specimens quenched at 1050°C.

3.1.2 Water + 100 ppm $FeCl_3$

Pickett, et al.[24] have reported several solutions that produce intergranular cracking of nonsensitized stainless steel. These included water solutions of $FeCl_3$, $FeCl_2$ $CuCl_2$, CrO_3, and NaOH at a temperature of

345°C. In these solutions cracking has been observed only on stressed specimens. It was found that the type of intergranular cracking produced in 100 ppm iron chloride water closely resembled the in-reactor cracking in appearance, and occurred over the same range of temperatures.

3.1.3 Fluoride Contaminated Water

Recent laboratory tests[13] have shown that Type 304 stainless steel is susceptible to intergranular fluoride icn (F^-) attack in neutral or alkaline water solutions. Extensive metallographic study of the corroded specimens demonstrated that F^- attack was purely intergranular and was limited to specimens with heavily sensitized structure. Neither the solution-annealed material nor the heat effected zone adjacent to weldment produced any trace of F^- attack under the same testing conditions. The attack was consistently less severe on sensitized material of finer grain size and/or lower carbon content. Specimens of other materials appeared to be completely resistant to F^- attack after a sensitizing heat treatment at 1150°F (621°C) for from 10 to 24 hr. These include Inconel 600, Incoloy 800, fine-grain Type 304 stainless steel, fine-grain Type 347 stainless steel, and austeno-ferritic weld deposits or castings. Attack occurred at room temperature and was more rapid at 82°C (180°F). Data are not yet sufficient to define the F^- concentration necessary for attack to occur. However, in a number of tests at 180°F, concentrations less than 1 ppm F^- in bulk solution caused slight attack in crevices. A very high concentration (4 wt% NaF) was not corrosive. The rate and mode of F^- attack was not affected by the amount of Cl^- in the corrosive solution over a range from about 15 ppm to less than 30 ppb. With respect

to possible mechanistic interpretation, the following patterns are significant:

1. Cracking occurs at room temperature.
2. Wide changes in the pH have no effect (pH range tested 4.70-10.45).
3. Very high F^- concentrations stop cracking.
4. Intergranular attack *without* stress occurs with air formed oxide; whereas, intergranular attack on oxide free surface occurs only *with* stress (except in crevices).

3.1.4 Water + 100 ppm Oxygen

General Electric Co. at Vallecitos used a bellow-loading system to study the intergranular cracking on austenitic stainless steel in water containing 100 ppm oxygen at a temperature of 289°C (554°F).[25,26] The tensile specimen was stressed by adjusting the load to 0.2% offset yield strength (at 289°C). The materials used in this study include Type 304 stainless steel (0.07 C) Type 304L stainless steel (0.02 C), 304 + Si (0.07 C, 4.1 Si), nickel doped 304 + Si (0.06 C, 4.0 Si, 14.3 Ni), U. S. Steel 18-18-2 (0.06 C, 1.92 Si), Uranus S (0.02 C, 4.2 Si 13.9 Ni, 17.6 Cr) and Uranus-50 (0.05 C, 0.51 Si, 7.9 Ni, 20.3 Cr). Three heat treatments were employed:

i) Solution annealed at 1095°C (2000°F) and water quenched
ii) Sensitized, 24 hr at 595°C (1090°F) in vacuo and furnace cooled
iii) As welded.

No evidence of localized attack was found after 300 hr of exposure, when tested in the solution-annealed condition. In the sensitized condition, only those austenitic alloys (e.g., Type 304 stainless steel, nickel doped 304 + Si and U. S. Steel 18-18-2) with continuous sheet-type carbides in the grain boundaries exhibited cracking in 17-23 hr. Other austenitic alloys (e.g., Type 304L stainless steel and Uranus S) that were relatively free of continuous sheet-type carbides in the grain boundaries or duplex structure alloys (austenite + ferrite - e.g., Type 304 stainless steel + Si and Uranus-50) with no carbide precipitation in the austenite grain boundaries showed no failure in the 300-hr test. To explore further the intergranular stress-corrosion behavior of sensitized austenitic alloys of varying carbon content, a series of carbon-doped, high-purity alloy (18 wt% Cr-9 wt% Ni), with from 0.02 to 0.15 wt% carbon, was likewise tested in the sensitized condition. The time-to-failure decreased rapidly when the carbon content exceeded 0.03 wt%. In addition, sensitization behavior of welded heavy plate section of Types 304 and 304L stainless steel was evaluated. The welds were made on 0.5-in.-thick plates (6 by 6 in.) by using a shielded argon-arc process employing 3 passes at high heat input with Type 308 stainless steel filler material. Tensile specimens were then cut from the plate welds that have the weld bead in the middle of the gage section. Duplicate specimens of a Type 304 stainless steel weld failed in 40 and 45 hr, and corresponding specimens of a Type 304L stainless steel weld survived in similar stress-corrosion tests for the entire period of 300 hr. Metallographic examination revealed the intergranular cracking

occurred through a region of heavy carbides 0.25 in. from the Type 304 stainless steel weld bead. The Type 308 stainless steel weld displayed no cracking nor was carbide precipitation visible, as in the case of the Type 304L stainless steel weld bead.

The following conclusion may be drawn from the above work:

1. Solution-annealed material with no plastic deformation, other than that associated with stressing to yield point, showed no evidence of intergranular stress corrosion after exposure to 289°C water + 100 ppm O_2.
2. Sensitized austenitic materials ($C \leq 0.03$ wt%) do not exhibit intergranular stress corrosion in the above environment.
3. Addition of Si to the austenitic alloy is of no benefit, if the carbon content is sufficiently large to cause carbide precipitation during sensitization.
4. Duplex alloys (ferrite + austenite) appear to be immune to intergranular stress corrosion even after a heat treatment that would normally result in sensitization in austenitic materials. This immunity is independent of the nature of the ferrite stabilizer employed.

Recently, Wilde[27] evaluated kinetics of crack initiation of sensitized Type 304 stainless steel. He observed:

(a) the induction time (T_N) for cracking increases markedly when applied stress decreases from 30,000 to 20,000 lb/sq. in., and

(b) cracking appears to nucleate in the plastically deformed area of the surface.

In addition, surface pickling with HNO_3-HF on Type 304 stainless steel after sensitization (at 621°C (1150°F) for 12 hr) lowers the cracking period from 5 to 10 times compared with corresponding sensitized specimens without HNO_3-HF pickling. It should be pointed out that this surface treatment may be related to F^- attack.[13] However, crevices produced at the grain boundary by pickling is not a likely factor in the absence of F^-. For example Armijo[25] pickled solution-annealed specimens of Type 304 stainless steel in a boiling nitrate-chromate solution to produce deep ($\sim$0.015 cm), uniform, intergranular corrosion at the specimen surface. The specimen was then washed in boiling water and no stress corrosion failure occurred in the 289°C water + 100 ppm oxygen test.

3.2 Irradiation Embrittlement

Hydrogen and helium, which can embrittle austenitic stainless steel, are known to be present in the nuclear reactors. Hydrogen is generated from radiolytic dissociation of water in thermal flux reactors. Hydrogen is also produced by transmutations in (n,p) reactions in the matrix elements (Fe, Ni, and Cr) of austenitic stainless steel. Similarly, helium is formed by transmutations in residual boron and in the (n,α) reaction in the matrix elements. Helium is currently considered a major cause of irradiation embrittlement in fast breeder reactors, but not in water-cooled reactors. In the latter case, the operating temperature is too low for grain-boundary shearing. For this reason only hydrogen embrittlement will be discussed.

3.2.1 Hydrogen Embrittlement

Whiteman and Trorairo[28,29] showed that thin sections of cathodically hydrogenated austenitic stainless steel suffered a significant loss of ductility in analogy with well-characterized hydrogen embrittlement of ferritic steel. A similar result was observed by Cheng[11] and by Vennett and Ansell[30] on Type 304L stainless steel when tested in a high-pressure hydrogen atmosphere.

4. Mechanisms of Intergranular Corrosion Cracking

In virtually all known cases of intergranular brittleness, it can be shown that the brittleness is associated with the presence of some impurity. Presumably, the impurity is present in the narrow grain-boundary interface in much higher concentration than the mean composition of the metal would indicate.[31] There has been for many years qualitative evidence for segregation of solutes to grain boundaries. This evidence has been reviewed by Inman and Tipler[32] in 1963, and by Westbrook[33] in 1964.

In the past year or so, two new quantitative techniques have emerged to study the structure and composition of the grain boundaries. Marcus and Palmberg[34] used Auger Electron Spectrometry to study antimony segregation at the intergranular fracture surface of embrittled AISI 3340 steel. Brenner et al.[31,35] are using field ionization atom probes to explore atomic structure at a grain boundary and to identify the individual atoms in that structure.

4.1 Solute-Segregation Theory

In nitric-dichromate solution, Aust[36] postulated that chemical concentration differences exist between grains and grain boundaries, that is, impurity segregation at boundaries. These chemical differences provide the driving force for localized attack. It is this impurity segregation that can lead to accelerated dissolution of grain boundaries when the alloy is exposed to a suitable corrodant. Thus, a rather simple model for intergranular corrosion is shown schematically in Fig. 1. It was proposed[37] that the intergranular corrosion of austenitic stainless steel is associated with the presence of continuous grain-boundary paths of either solute-segregated (e.g., phosphorus) or second-phase (carbide) regions. For Type 304 stainless steel in the solution-treated condition, that is, quenched from 1050° to about 1300°C, the solute segregation at the grain boundaries provides a narrow continuous path for attack by the corrosion solution, as shown in Fig. 1(a). If the austenitic stainless steel is quenched from 600°C (or from the sensitization heat-treatment range of 500 to 700°C), continuous carbides or second phase regions are formed at the grain boundaries, Fig. 1(b), thereby producing a wide continuous path for classical intergranular corrosion in the sensitized condition. In material heat treated and quenched from 800 to 900°C, isolated carbides may incorporate solute impurities drained from the grain-boundary region. This latter heat treatment (i.e., quench from 800 to 900°C) should then reduce the intergranular corrosion rate, since a discontinuous penetration path for the corrosion medium is now present at the grain boundaries. In addition the reduced corrosion rate should

remain unchanged even after subsequent 150 hr sensitization at 650°C. The reason is that carbide precipitation at 850°C should reduce the carbon supersaturation sufficiently to prevent further nucleation of the carbide at the lower temperature of 650°C, despite the decrease in the solubility of the carbon at the lower temperature. Also on the basis of this model, a low corrosion rate would be expected for a high-purity material having relatively clean or segregation-free grain boundaries, as shown in Fig. 1(d). The results of the Aust et al.[36,38] investigation in nitric-chromate solution clearly supported this model.

According to the chromium-depletion theory, the beneficial effect of a stabilization heat treatment (800 to 900°C) on corrosion of austenitic stainless steel is due to the diffusion of chromium into the chromium-depleted areas adjacent to the precipitated carbides. However, as was shown previously when Type 304 stainless steel is slowly cooled from 1300 to 900°C, held for 1 hr at 900°C and quenched, a high rate of intergranular attack is still observed. In other words, at the same annealing temperature and time where chromium diffusion is thought to remove chromium-depleted regions, poor corrosion resistance is found, which is due to the observed continuous carbides present at the grain boundaries.[39] This result is in agreement with the Aust model[37] but not with the chromium-depletion theory.

One of the important problems remaining was to determine the identity and state of the solute segregation that was involved in the intergranular corrosion of solution-treated and quenched austenitic stainless steel. The fact that some type of solute segregation is responsible is

indicated by the work of Chaudron[40] who found that high-purity stainless steel is immune to grain-boundary corrosion in boiling nitric-dichromate solutions. The recent results by Hanneman and Aust[38] have suggested that the mechanism of nonequilibrium solute segregation induced by excess vacancies may also be responsible for intergranular corrosion of solution-treated and quenched austenitic stainless steel. For example, both excess grain-boundary hardening (Fig. 2) and intergranular corrosion are observed in solution-treated Type 304 stainless steel. However, when a high-purity austenitic stainless steel containing no excess grain-boundary hardening[41] is tested, there is no evidence of intergranular corrosion.[22] In addition, it is found[22] that a solute such as phosphorus (0.01-0.1 wt%) promotes susceptibility to intergranular corrosion of solution-treated, high-purity austenitic stainless steel in nitric-dichromate solutions, whereas carbon (up to 0.1 wt%) has little effect (Fig. 3). The boundary hardening is found with carbon additions, except in the highest carbon alloy tested. Electron microscopy examination revealed the presence of carbide at the grain boundary.[38]

Finally, the solute-segregation theory of intergranular corrosion of austenitic stainless steel is useful in analyzing the service failures in water-cooled reactors (Section 2) and in aqueous solution tests (Section 3). The only differences among these corrodents are rate of intergranular attack. In the case of duplex alloys (ferrite + austenite) in water + 100 ppm oxygen tests (Section 3.1.3), it has been reported[42] that the carbon precipitates at the ferrite/austenite boundaries and

reduces the availability of carbon for precipitation of the austenite/austenite boundaries. Thus, the latter boundaries probably have "stabilized" or "segregated" structures rather than "sensitized" structures.

4.2 Hydrogen Induced Transformation

The mechanism of hydrogen embrittlement in austenitic stainless steel due to a hydrogen-induced transformation was recently elucidated by Whiteman[29] and by Holzworth and Louthan.[43] Cathodic hydrogenation of austenitic stainless steel led to partial transformation of the γ (fcc) austenitic lattice to the martensitic phases, α' (bcc) and ε (hcp). The latter phases were the same as those formed by cold working hydrogen free austenite at very low temperatures. Whiteman further showed that absorption of hydrogen led both to internal strain, induced by an expansion of the γ (fcc) lattice, and to a significant lowering of the stacking-fault energy (related to the activation energy barrier inhibiting phase transformation). As a consequence, the martensitic transformation was induced even in normally stable Type 310 stainless steel (20% Ni, 25% Cr), which normally does not undergo a strain-induced martensitic transformation even at -4 K. Benson et al.[44] have further shown that brittle intergranular fracture occurs along martensitic platelets formed in the presence of hydrogen atmosphere. These results indicate that the presence of hydrogen causes embrittlement and initiates microcracks at the strain-induced martensitic platelets in the steel.

Conclusions

Nuclear pressure vessels, primary piping, core components, and fuel-element cladding are subject to cyclic thermal and mechanical stresses due to the high pressure and temperature of the coolant or of the fuel. When Type 304 stainless steel is used as material for these parts in water-cooled reactors, instances of intergranular corrosion failure due to the combined action of corrosion and low-cyclic stress or high static stress have been occasionally observed.

Sensitization is not a prerequisite for intergranular corrosion of Type 304 stainless steel. Under certain conditions, solution-annealed Type 304 stainless steel will behave likewise. This is evidenced by the service failures in water-cooled reactors and by test results in laboratory corrosion studies.

Based on the solute-segregation theory, Aust[41] postulated that intergranular corrosion of austenitic stainless steel is associated with localized attack on the impurities segregated at the grain boundaries. This is the reason that a sensitized condition, which has a wide continuous path of either solute-segregated (e.g. phosphorous) or second phase (carbide) regions, is more susceptible to intergranular corrosion cracking than a solution-annealed condition with a narrow continuous path of segregates. Similarly, a stabilized condition with a discontinuous path of isolated carbide is expected to be even less susceptible to intergranular corrosion cracking. A high-purity material that has relatively clean or segregation-free grain boundaries is immune to such cracking.

The presence of hydrogen can cause embrittlement and also initiates microcracks at the strain-induced martensitic platelets in Type 304 stainless steel.

The intergranular corrosion failures of Type 304 stainless steel in water-cooled reactors may be related to (a) selective chemical attack of impurities segregated at grain boundaries or (b) hydrogen embrittlement, or both.

References

(1) W. H. Arlt and S. R. Vanderberg, Gen. Elec. Co. Report GEAP-4360 (1963).

(2) C. N. Spalaris, Nucleonics, 21, p. 41 (1963).

(3) J. P. Higgins, Nuclear News, Nov., p. 37 (1968).

(4) N. Balai, C. R. Sutton, E. A. Winunc, and R. F. Jones, Argonne National Laboratory Report ANL-7117 (1965).

(5) T. J. Pashos, TID-8540 (1964).

(6) S. R. Rideout, Savanah River Laboratory Report DPSPU 62-30-26 (1963).

(7) R. N. Duncan et al., Nuclear Applications, Vol. 1, No. 5, p. 413 (1965).

(8) S. Naymark and C. N. Spalaris, International Geneva Conference on Peaceful use of Atomic Energy, Vol. 11, p. 432 (1964).

(9) W. S. Hazelton, C. J. Kubit and D. R. McClintock, Trans. Am. Nucl. Soc. Vol. 6, No. 2, p. 388 (Nov. 1963).

(10) D. C. Bullington, USAEC Report YAEC-182, (Jan. 1962).

(11) C. F. Cheng, Corrosion, p. 341 (Nov. 1964). & unpublished data.

(12) W. E. Berry, Reactor Materials, Vol. 7, No. 1, (1964).

(13) C. T. Ward, D. L. Mathis and R. W. Stachle, Corrosion, p. 394 (1969).

(14) W. B. DeLong, ASTM Spec. Tech. Pub. No. 93, p. 211 (1949).

(15) H. T. Shirley and J. E. Trumann, Jn. Iron and Steel Inst., Vol. 171, p. 304 (1952).

(16) A. B. McIntosh, Chemistry and Industry, p. 667 (1957).

(17) J. E. Truman, Jn. Appl. Chem., Vol. 4, p. 273 (1954).

(18) M. A. Stretcher, J. Electrochem. Soc. Vol. 106, p. 161 (1959).

References

(19) H. Coriou et al., Colloque de Metallurgy IV, p. 75 (1960).

(20) J. S. Armijo, Corrosion, p. 235 (1965).

(21) M. Warzee and P. Berge, Comptes Rendons, Vol. 259, p. 144 (1964).

(22) J. S. Armijo, Corrosion, p. 24 (1968).

(23) K. T. Aust, Trans. of Met. Soc. of AIME, Vol. 245, p. 2117 (Oct. 1969).

(24) A. E. Pickett et al., Nuclear Applications, Vol. 1, No. 5, p. 453 (1965).

(25) J. S. Armijo, Corrosion, p. 319 (1968).

(26) Jersey Central Power and Light Co., USAEC Docket No. 50-219, Amendment No. 37, Reactor Vessel Repair Program - Oyster Creek Nuclear Power Plant No. 1 (April 1968).

(27) R. E. Wilde, Corrosion, p. 359 (1969).

(28) M. B. Whiteman. PhD.Thesis. Case Inst. of Tech. (1965).

(29) M. B. Whiteman and A. R. Trorano, Corrosion, p. 53 (1965).

(30) R. M. Vennett and G. S. Ansell, Trans. ASM, Vol. 60, p. 242 (1967).

(31) J. R. Low, Trans. TMS-AIME, Vol. 245, p. 2481 (1969).

(32) M. C. Inman and H. R. Tipler, Met. Review, Vol. 8, p. 105 (1963).

(33) J. H. Westbrook, Met. Review, Vol. 9, p. 415 (1964).

(34) H. Marcus and P. W. Palmberg, Trans. TMS, Vol. 245, p. 1664.

(35) S. S. Brenner and J. Y. McKinney, Appl. Phys. Letters, Vol. 13, p. 29 (1968).

(36) K. T. Aust, TMS-AIME, Vol. 245, p. 2117 (1969).

(37) K. T. Aust, J. S. Armijo, and J. H. Westbrook, ASTM Trans. Quart., Vol. 59, p. 544 (1966).

(38) R. E. Hanneman and K. T. Aust, Scripta Met. Vol. 2, p. 235 (1968).

(39) K. T. Aust, J. S. Armijo, E. F. Koch and J. H. Westbrook, ASM Trans. Vol. 60, p. 360 (1967).

(40) G. Chaudron, EURAEC-796, Quart. Report 6, Oct.-Dec. (1963).

(41) K. T. Aust, J. S. Armijo, E. F. Koch and J. H. Westbrook, ASM Trans. Quart. Vol. 61, p. 270 (1968).

(42) Metals Handbook, 1, Properties and Selection of Metals, 8th Edition, p. 435 (1961).

(43) M. L. Hozworth and M. R. Louthan Jr., Corrosion, p. 110 (1968).

(44) R. B. Benson Jr., R. K. Dann and L. W. Roberts, Jr., Trans. Met. Soc. AIME 242, p. 2199 (1968).

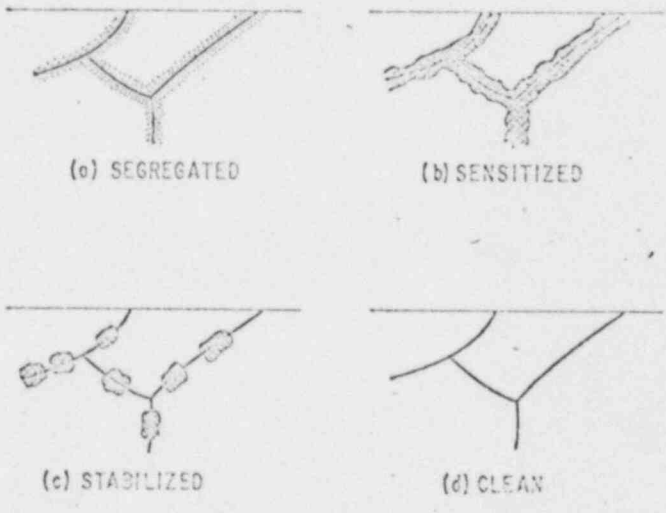

Fig. 1. Schematic illustration of the model proposed for intergranular corrosion.(41)

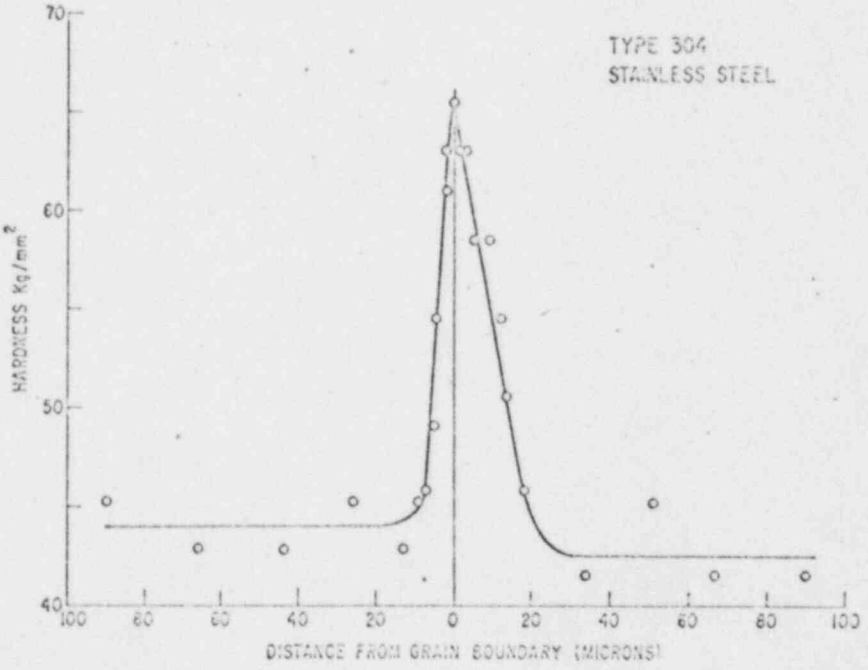

Fig. 2. Hardness-distance profile near a grain boundary in solution-treated Type 304 austenitic stainless steel (1-g load, 5-sec loading time).(45)

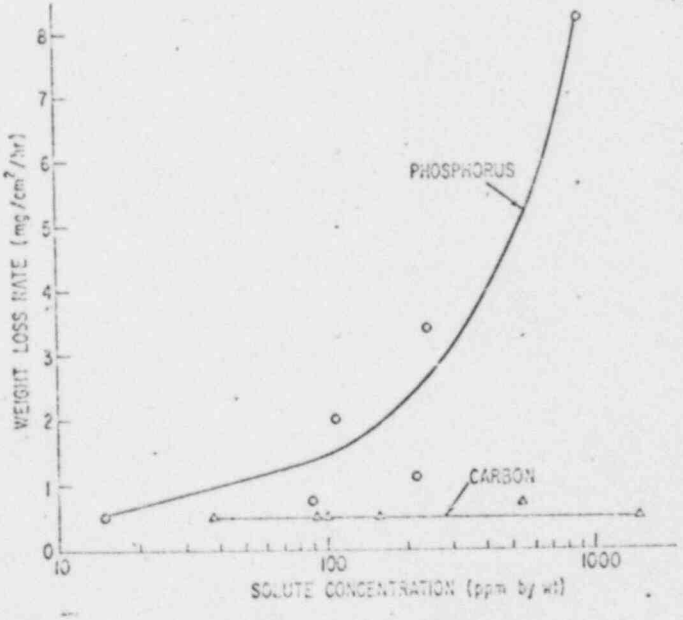

Fig. 3. Effect of phosphorus or carbon additions on the corrosion resistance of solution-treated high-purity austenitic stainless steel (14 wt% Cr, 14 wt% Ni, balance Fe) in boiling nitric-dichromate solution.(22)